



Study on the potential optimization of columns sizes in steel concentrically braced frames

Frédéric Daniel¹, Charles-Philippe Lamarche²

¹ M.A.Sc. Student, Department of Civil and Building Engineering, University of Sherbrooke - Sherbrooke, QC, Canada.

² Ph.D., Associate Professor, Dept. of Civil and Building Engineering, University of Sherbrooke - Sherbrooke, QC, Canada.

ABSTRACT

In this paper, a brief literature review of column behavior in concentrically braced frames (CBF) under seismic action is presented. The results of nonlinear time history dynamic analyses that were performed to study the interaction between the axial load and the bending moment developed in columns in a two stories chevron CBF structure are also presented and discussed. To conduct these analyses, artificial accelerograms were selected and calibrated. The study is based on a two-story chevron CBF building located in Vancouver that was sized according to the National Building Code of Canada (NBCC) and the CSA S16-14 standard. The building structure was modeled numerically using the finite element software OpenSEES. The results of the numerical analyses showed good agreement between the expected story drifts and the axial loads that developed in the bracing members when compared to the design values. Furthermore, the bending moment levels reached in the columns did not exceed 20% of the plastic moment of the column's section, which is the design value prescribed in CSA S16-14. However, the maximum interaction equation value involving the axial load and bending moment in the columns of the lateral force resisting system were 20 % lower than expected using CSA S16-14 interaction equation. This was due to asynchronous occurrences in time between the maximum axial load and bending moment in the columns.

Keywords: columns, chevrons, seismic, time-history, nonlinearity

INTRODUCTION

In Canada, low and medium height steel buildings are often used for commercial, industrial, and residential purposes. To withstand the forces induced by earthquakes, they must be equipped with an adequate lateral force resisting system (LFRS). Among those recognized by the CSA S16-14 standard [1], concentrically braced frames (CBF) are frequently used because of their relatively low construction cost and speed of erection. When significant lateral forces are induced by strong ground motions, bracings in CBFs must dissipate energy through inelastic deformations. When the braces in tension undergo inelastic deformations and the compression braces either undergo inelastic deformations and/or the braces buckle, the lateral stiffness of the building structure is significantly reduced and inter-story drifts are amplified. These inter-story drifts amplify the bending moments in the columns which can compromise the structural stability/integrity of the building. In this respect, the CSA S16-14 standard requires taking into account an additional bending moment equal to 20% of the plastic moment of the column's section when sizing columns part of the LFRS. Considering that this amplified bending moment may occur for a very short period of time and that it is unlikely that the maximum axial force developed in the columns appear at the same time, it is therefore legitimate to ask whether this additional bending moment could to be revised or simply neglected in design. In addition, it was demonstrated in the literature [2] that columns continuous over multiple stories have a greater strength because of continuity and the fact that the design axial loads are unequal from one story to the next. Because CSA S16-14 imposes that columns must be continuous over a minimum of two stories, the potential overstrength arising from this practice may be sufficient to counteract the potentially amplified bending moments.

LITERATURE REVIEW

Performance of CBFs under seismic loading

In a steel structure where the LFRS is a concentrically braced frames, the kinetic energy induced by a strong ground motion is essentially dissipated by the inelastic deformations in the bracing members, i.e. by the permanent deformations in the braces in tension and the flexural inelastic buckling of the braces in compression. Under cyclic loads such as earthquake loads, the bracing members are submitted to a succession of tension and compression episodes. The tension brace must sustain increasing loads up to its elastic capacity ($P_y = A_g F_y$), where P_y represents the maximum elastic load of the bracing member, A_g the gross area of the section of the member and F_y is the yield stress. After the attainment of P_y , the braces undergo irreversible deformations. When the load is reversed, the load decreases until the probable compression resistance C_u is reached. Assuming

a pinned-pinned condition ($K = 1.0$), a plastic hinge is expected to appear at midspan under compressive loads [3]. When reloaded in tension, the diagonal will reach its full capacity only if the maximum previous elongation is surpassed. In the subsequent cycles, the post-buckling capacity of the compression member C_u gradually diminishes as the out-of-plane residual deformations cumulate at each cycles and local buckling occurs in the plastic hinge region. Figure 1 shows the hysteretic response of a rectangular hollow section (RHS) brace submitted to a quasi-static displacement-controlled cyclic test.

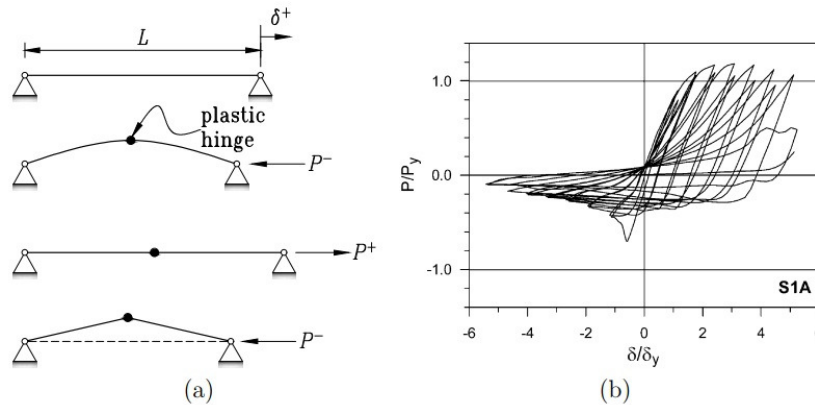


Figure 1. Displacement history of a RHS bracing member under cyclic loading: (a) expected displacements, (b) hysteretic behavior, adapted from [3].

Concentration of inelastic demand

For concentrically braced frame, researches conducted by Tremblay (2003) [4] have shown that diagonal bracing members possess a low capacity to divide adequately the inelastic deformations along the entire height of the structure. Thereby, the inelastic demand tends to concentrate in the stories where the shear demand is higher than the elastic resistance, i.e. at the upper and lower levels of the building structure. High inelastic shear demand tends to occur at these levels because of the shear amplification generated by higher modes of vibration (higher levels) and the presence of important gravity loads (inferior levels). This concentration of inelastic demand contributes to accentuate inter-story drift which amplifies the $P-\Delta$ effects. Because of that, the CSA S16-14 standard requires that columns in CBF must be continuous over a minimum of two story to help redistribute the inelastic demand and to ensure that a soft story mechanism does not appear. A graphical representation of the inelastic demand concentration is presented on Figure 2.

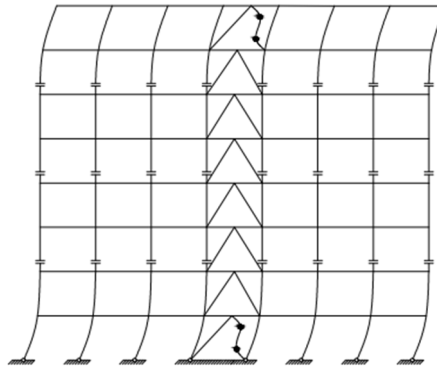


Figure 2. Flexural deformation of columns produced by the concentration of the inelastic shear demand.

CASE STUDY

A two stories steel building structure using a MD (moderately ductile) concentrically braced frame ($R_d = 3.0$ and $R_o = 1.3$) designed in accordance with NBCC 2015 [5] and the CSA S16-14 standard was designed. The capacity design principle involved in the design requires that the bracing members are sized to resist a combination of gravity and seismic loading. The columns and beams were designed to remain elastic as they must withstand the probable forces generated by the yielding and buckling of the bracing members. ASTM A500 Grade C steel was considered for the HSS bracing members and ASTM A992 steel for type W beams and columns. An elastic resistance of 345 MPa and an elastic modulus of 200000 MPa were considered for all the structural members. $P-\Delta$ effects and accidental torsion were considered at the design stage.

Building geometry

The two-story building structure is composed of an inverted V chevron braced frame. Both stories are 4 meters high. Each principle direction of the building is equipped with two CBFs located at half-length of each façade. The building is assumed to be located on a class C soil in the city of Vancouver. All columns were considered continuous over the building height with restraints conditions at each level preventing flexural-torsional buckling. Figure 3 shows the building structure's geometry along with the selected steel shapes.

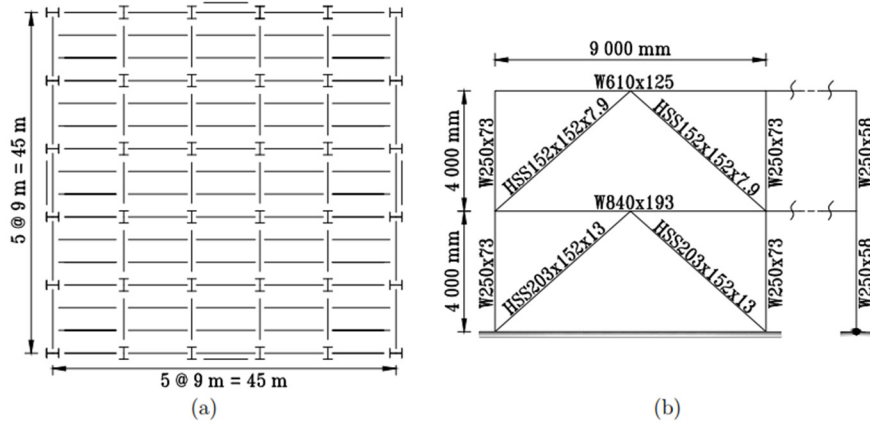


Figure 3. Building components: (a) plan view geometry, (b) elevation view with selected shapes.

NUMERICAL MODEL

The numerical analyses performed in this study have been modeled with the finite element software OpenSEES [6]. To simplify the model, only one LFRS bay of the building shown in Figure 3 was modeled. Six degrees of freedom (DOF) have been considered for the 3D analyses. Beams that were not part of the LFRS were omitted and replaced by kinematic constraints between the gravity and LFRS columns. The initial out-of-straightness and residual stress of the diagonals and columns were considered.

Finite element representation

Diagonals, beams and columns were modeled using force based nonlinearBeamColumn elements. Height elements with four integration points were used to model the columns over each story. Both LFRS and gravity columns had their cross-section discretized with 50 fibers using the Steel02 material. An out-of-straightness of $\delta_0 = L/1000$ was assumed at column mid-height to obtain a half-sine wave initial deformation. Gravity columns were connected to the LFRS by assigning a slave/master node at every level. The residual stress pattern proposed by Galambos and Ketter (1959) [7] and shown on Figure 4 was adopted.

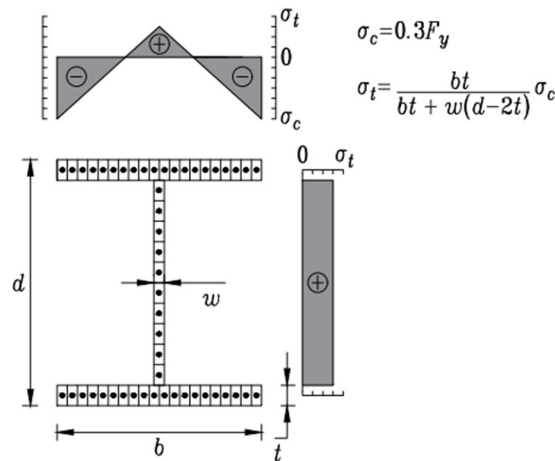


Figure 4. Residual stress pattern with discretized cross-section for column elements.

where b represents the flange width, t the flange thickness, w the web thickness, d the web depth, σ_t the residual tension stress at the middle of the flange and lastly σ_c the residual compression stress at the tip of the flange. Diagonals were also modeled using height elements with four integration points. The cross-section was discretized using 20 fibers [8] and initial out-of-

straightness of $\delta_0 = L/300$ was considered to better represent design assumptions regarding the compression strength. Beams were modeled with six elements with four integration points per element. Each cross-section was discretized using 50 fibers. Connections between the beams and columns were modeled with rigid links by using a stiff elastic beam element. The flexibility of the gusset plates was modeled using a nonlinear spring element (zero length element) having user specified rigidity values for out-of-plane flexure and torsion. Connections between the beams and braces modeled similarly. Figure 5 illustrates the finites element model used for modeling of the LFRS frame and the braces connections.

Structural analysis

A static modal analysis was performed including the gravitational loads to evaluate the eigen periods of the building structure ($T_1 = 0.426$ s and $T_2 = 0.181$ s). Hereafter, nonlinear dynamic analyses were conducted to better understand the behavior of steel CBF columns under strong ground motions. These nonlinear incremental analyses were performed using Newmark average acceleration integration scheme with Newton iterations to reach convergence using $\Delta t = 0.001$ s. The Rayleigh damping matrix C used was considered proportional to the mass matrix M and the initial stiffness matrix K_0 of the structure with 3 % critical damping for the first two modes of vibration.

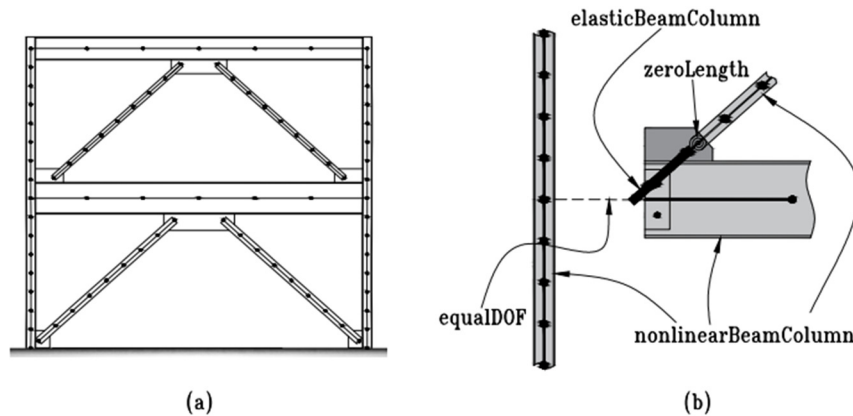


Figure 5. OpenSEES model: (a) LFRS frame, (b) brace connection.

Ground motions

The stochastic finite-fault method procedure proposed by Atkinson [9] to generate earthquake time histories that may be scaled to match the NBCC uniform hazard spectrum (UHS) has been employed for this exploratory study. The five artificial ground motions selected for the city of Vancouver were scaled to the NBCC UHS (2 % exceedance probability in 50 years) for a period range of interest lying between 0.1 s and 0.5 s. Figure 6 presents the calibrated ground motions with a focus on periods of interest.

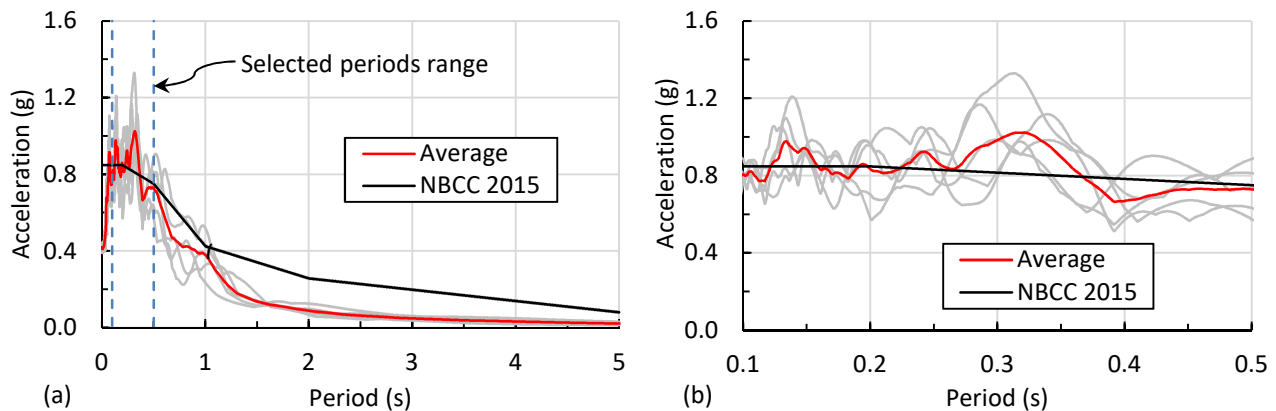


Figure 6. Acceleration response spectrums calibrated for the city of Vancouver: (a) $0.0 \leq T \leq 5.0$ s, (b) $0.1 \leq T \leq 0.5$ s.

RESULTS

This section presents the results of a two-story chevron steel braced frame building subjected to five design level ground motions calibrated for the city of Vancouver’s UHS. These analyses aimed to study the behavior of LFRS columns subjected to complex interaction between axial forces and bending moments.

Story drift

The inter-story drift history obtained from the most severe of the five accelerograms is plotted in Figure 7, where the inter-story drift at each story remained within the limits prescribed by NBCC (2.5 % of h_s for a building of the “normal importance” category with $I_E = 1.0$, where h_s is the story height and I_E the importance factor). The figure also shows that the lateral displacements at both levels are generally in phase, which suggests that the response of the structure was governed by its fundamental mode of vibration. This leads to believe that the maximum story shear occurred in the same direction for the two stories, as assumed at the design stage. At the end of the ground motion, one can also observe that both stories are oscillating around novel positions of equilibrium that shifted away from the initial zero positions. This confirms that the bracing members went through inelastic deformations which resulted in permanent residual story drifts.

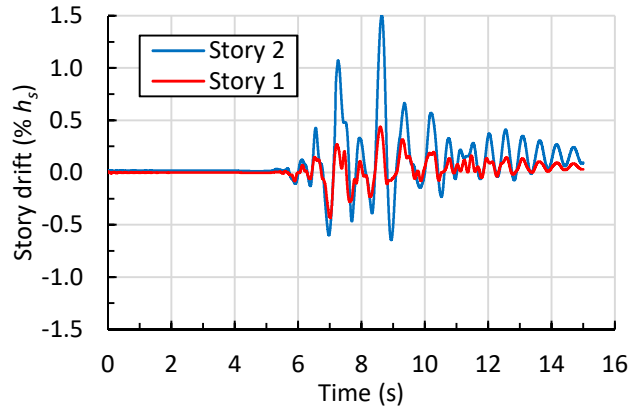


Figure 7. Story drift in function of time.

Axial loads in the CBF columns

According to the capacity design principle, it is expected that LFRS columns remain within the elastic range while resisting the maximum probable forces transferred by the energy dissipation elements. To confirm that this design principle was fulfilled during the simulations, Figure 8 presents the axial load history in the LFRS columns that occurred during the most severe earthquake simulation. In this Figure, compression forces are expressed as positive and tension forces are expressed as negative in sign. At the design stage, the maximum factored axial load expected in the LFRS columns were 390 kN and 1400 kN, for the 2nd and 1st story, respectively. As depicted on Figure 8, the peak values obtained in the simulations are in good agreement with design values. The average relative difference between the peak compression value obtained from the five simulations and the design value is +3.04 % for story 2, and -4.56 % for story 1. In all simulation cases, the columns did not buckle and remained in the elastic domain. The hysteresis curves of the columns axial force vs axial deformation, not presented herein, confirmed this fact.

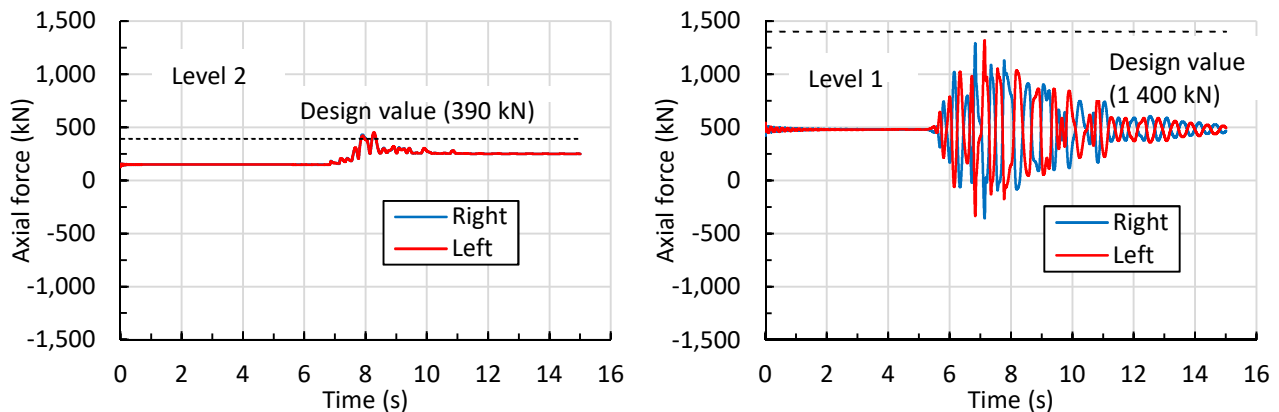


Figure 8. Axial load in the CBF columns for each story in function of time.

Axial loads in the bracing members

Figure 9 is plotted to compare the axial loads developed in the bracing members during the strongest imposed ground motion with the design values. In this Figure, compression forces are expressed as negative and tension forces are expressed as positive

in sign. The time histories show that the peak tension and compression loads reached during the analyses are in good agreement with the expected design loads. Average maximum responses obtained are 8.35 % different for story 2 and 2.21 % for story 1.

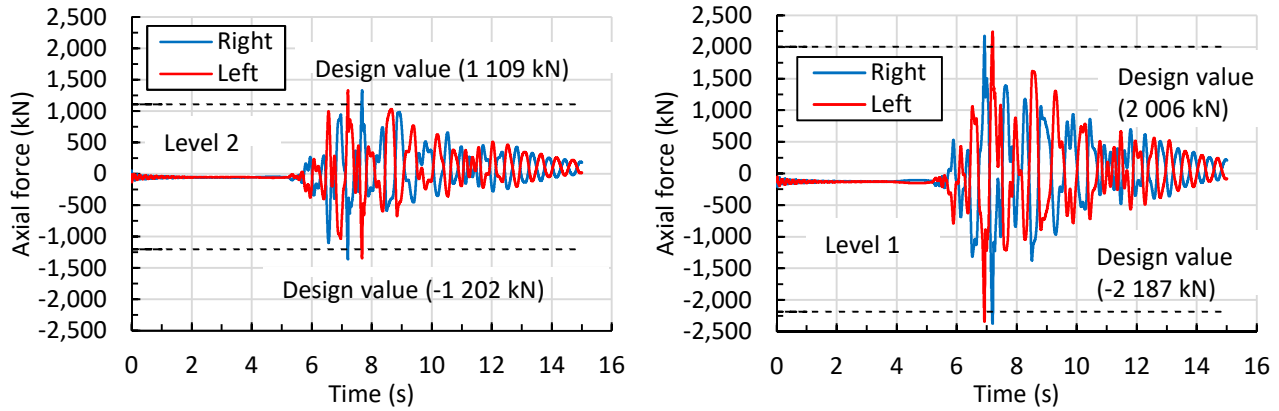


Figure 9. Axial load in the bracing members at each story as a function of time.

Bending moments in the columns

As discussed in the previous sections, concentration of inelastic shear demand is likely to introduce non-uniform inter-story drift that amplifies the bending moments in the columns. Figure 10 shows the maximum bending moment values recorded in the columns for the most severe accelerogram. In average, the bending moments observed were a little lower than $0.2M_p$ for both the LFRS columns and the gravity columns. The bending moments observed in the simulations are in good agreement with those put forward by CSA S16-14. In the case of the gravity columns, the reduced factored gravity loads assumed to be present in design yields to some reserve capacity, and therefore, the additional bending moment $0.2M_p$ can be ignored at the design stage as prescribed by CSA S16-14.

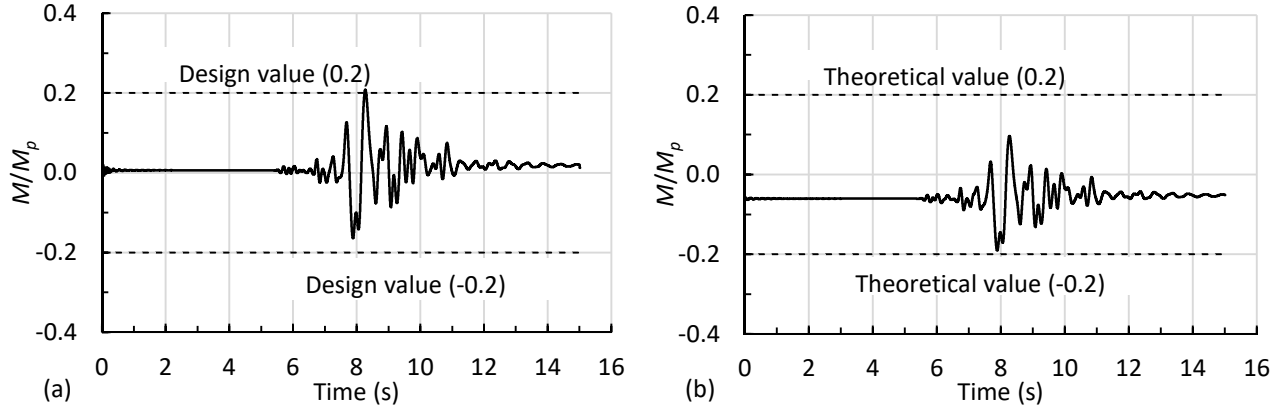


Figure 10. Bending moment in function of time: (a) LFRS column, (b) gravity column.

Interaction

The CSA S16-14 requires that beam-column members in CBFs must resist combinations of axial compressive force and bending moment. The corresponding interaction equation to evaluate beam-column resistance is:

$$\frac{C_f}{C_r} + \frac{0.85U_{1x}M_{fx}}{M_{rx}} + \frac{\beta U_{1y}M_{fy}}{M_{ry}} \leq 1.0 \quad (1)$$

where C_f is the factored axial load; C_r is the factored axial resistance; U_{1x} and U_{1y} are coefficients taking into account the P - δ effects about the strong and weak axes; M_{fx} and M_{fy} are the factored bending moments about the strong and weak axes; M_{rx} and M_{ry} are the factored bending moment resistance about the strong and weak axes; and β is a factor considering the effect of distributed plasticity on the stability. In this study, columns were subjected to axial loading and weak-axis bending only (see plan view in Figure 3a). Furthermore, columns were laterally braced at mid-height so that failure by lateral-torsional buckling was prevented about the strong axis. To review this complex dynamic interaction, ratios about axial loading and bending moment corresponding to Eq. (1) have been plotted as a function of time (Figure 11).

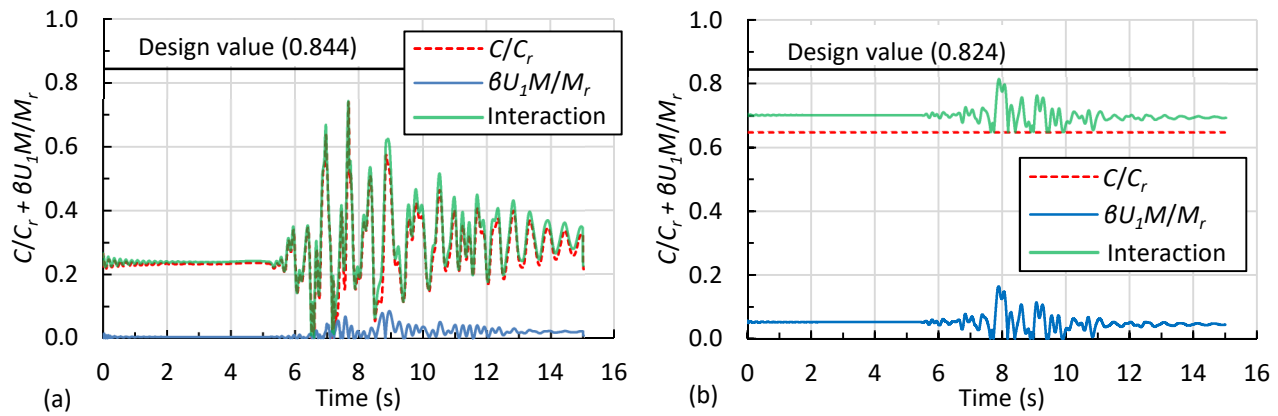


Figure 11. Interaction between axial load and bending moment as a function of time: (a) LFRS column, (b) gravity column.

For the LFRS column case, it is obvious that the axial load dominates the response and controls the time-history maximum interaction response. For the five analyses performed, an average maximum interaction of 0.767 has been observed when adding the two maximums ratios occurring at different instants. This 9.12 % difference with the design value (0.844) may be attributed to the slight differences between the response spectrums of the calibrated ground motions at the selected periods range and the UHS of NBCC 2015 (Figure 6b). On the other hand, when comparing the average maximum superposition response obtained with the design value, a 21.21 % difference is observed. This greater difference shows that axial loading and bending moment do not tend to occur simultaneously in the LFRS columns during a strong ground motion. In the case of the gravity columns (Figure 11b), one can see that the axial loads remain constant for the entire duration of the analysis. Therefore, the maximum bending moment evidently occurs at the same instant as the maximum axial load. Considering all five analyses, an average maximum interaction of 0.787 was observed, which is about 4.49 % lower than the design value (0.824). Even if this difference is small compared to the design value, structural integrity was never compromised because the gravity load case was more critical than the seismic load case at the design stage.

Discussion

In general, the additional maximum bending moments observed in the analyses were in accordance with the $0.2M_p$ value imposed by the CSA S16-14 Standard. When it comes to studying the maximum interaction between the axial loading and the bending moment, the results are somehow different. This may be explained by taking a closer look at the axial load and bending moment response during the time history analyses. Figure 11 shows that the first mode of vibration contributes in a more significant way to the axial force generated in the columns and that the second mode of vibration contributes more to the bending moment demands. Indeed, the first mode of vibration accentuates the compression force on the LFRS columns while the second mode of vibration presents a very high curvature at mid-height (Figure 12). Because these modes of vibration do not share the same natural frequency, it is unlikely that the maximum axial load and bending moment occur at the same instant.

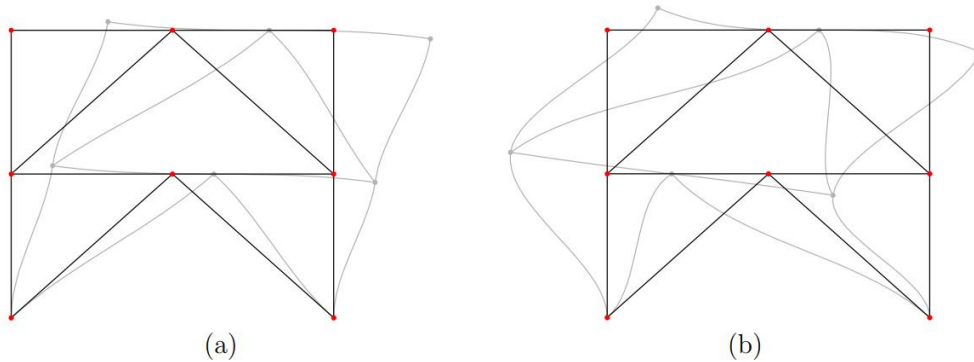


Figure 12. Modes of vibration obtained from LAS software: (a) First, (b) Second.

CONCLUSIONS

In this paper, a literature review on the seismic performance of CBFs and concentration of inelastic shear demand was first presented. A two-story steel building using a MD concentrically braced frame was designed according to the capacity design principles. Exploratory incremental nonlinear dynamic analyses were performed with the OpenSEES software to study the complex interaction of axial loading and bending moment. Five artificial design level ground motions were used and calibrated

to the UHS of the city of Vancouver. Preliminary results of the numerical simulations confirmed the adequacy of the design assumptions and validated the CSA S16-14 provisions regarding additional bending moments developed in columns during a design level earthquake. Response time histories showed that the building structure remained stable and maintained its structural integrity at all time. The average maximum interaction between axial loading and bending moment in the LFRS columns was found to be 21.21 % lower than the design value. This difference is attributed to the fact that axial loads and bending moment in the columns are not mainly influenced by the same vibration modes of the structure. Considering that previous studies [2, 10] have shown the presence of compressive overstrength in continuous columns in multi-storey building structures, further studies should be carried out to explore the possibility of code relaxation regarding columns requirements of CBFs steel structures. Probabilistic structural collapse assessment studies will be conducted based on the preliminary results presented in this study.

ACKNOWLEDGMENTS

The financial support from the Fonds de recherche du Québec – Nature et technologies (FRQNT) of the Québec Government, Canada, and the Natural Sciences and Engineering Research Council of Canada (NSERC) is acknowledged.

REFERENCES

- [1] Canadian Standard Association - CSA (2014). *CAN/CSA-S16: Design of steel structures*. Prepared by the CSA, Mississauga, ON.
- [2] Lamarche, C.-P., and Tremblay, R. (2010). “Experimental and numerical study on the potential for column size reduction in capacity designed multi-storey braced steel frames”. In *10th Canadian Conference on Earthquake Engineering*, Toronto, ON, Canada.
- [3] Tremblay, R. (2002). “Inelastic seismic response of steel bracing members”. *Journal of Constructional Steel Research*, 58(5-8), 665-701.
- [4] Tremblay, R. (2003). “Achieving a stable inelastic seismic response for multi-storey concentrically braced steel frames”. *Engineering Journal*, American Institute of Steel Construction, 40, 111-129.
- [5] National Research Council – NRC (2015). *National Building Code of Canada*. Prepared by the NRC, Ottawa, ON.
- [6] McKenna, F., Fenves, G. L., and Scott, M. H. (2000) “*Open system for earthquake engineering simulation*”. University of California, Berkeley, CA.
- [7] Galambos, T. V. and Ketter, R. L. (1959) “Columns under combined bending and thrust”. *Transactions of the American Society of Civil Engineers*, 126(1), 1-23.
- [8] Aguero, A., Izvernari, C. and Tremblay, R. (2006) “Modelling of the seismic response of concentrically braced steel frames using the OpenSees environment”. *International Journal of Advanced Steel Construction*, 2(3), 242-274.
- [9] Atkinson, G. M. (2009). “Earthquake time histories compatible with the 2005 National building code of Canada uniform hazard spectrum”. *Canadian Journal of Civil Engineering*, 36(6), 991-1000.
- [10] Lamarche, C.-P., and Tremblay, R. (2008). “Accounting for residual stresses in the seismic stability of nonlinear beam-column elements with cross-section fiber discretization”. In *2008 Annual Stability Conference*, Nashville, TN.